Controllable preparation of CaF$_2$ transparent glass ceramics: Dependence of the light transmittance mechanism on the glass crystallization behaviour

Xiwang Miao[a], Zhitao Bai[b,a], Xiangtao Huo[a], Min Guo[a], Fangqin Cheng[c], Mei Zhang[a,c,*]

[a] School of Metallurgical and Ecological Engineering, University of Science and Technology Beijing, Beijing, 100083, PR China
[b] Central Research Institute of Building and Construction Co., Ltd, MCC Group, Beijing, 100088, PR China
[c] Shanxi Collaborative Innovation Centre of High Value-added Utilization of Coal-related Wastes in Shanxi University, Taiyuan, 030006, PR China

ARTICLE INFO

ABSTRACT

Transparent glass ceramics containing CaF$_2$ nanocrystals were synthesized using a conventional melting and heat treatment process. The mechanism associated with the maintenance of the high transparency of the as-prepared glass ceramics was further clarified. The maximum light transmittance of the as-obtained transparent glass ceramics was approximately 85%, with microhardness value that reaches 761.62 ± 7.93 HV. To obtain transparent glass ceramics, in addition to controlling the CaF$_2$ nanocrystal size to be smaller than the wavelength of visible light, the average grain spacing (or concentration) of the CaF$_2$ is also a key factor. CaF$_2$ transparent glass ceramics were prepared following heat-treatment at a temperature between 630 °C and 700 °C for a period of 1–4 h; herein, the CaF$_2$ grain size was approximately 10–25 nm. The transmission electron microscopy (TEM) results showed that the CaF$_2$ grains were evenly distributed within the glass phase and that the average grain spacing was greater than 5.64 nm. The Raman analysis results indicate that at 730 °C, there was a significant increase in the degree of polymerization and an obvious increase in the concentration of CaF$_2$ grains. The average grain spacing was much lower than 5 nm, and therefore, light energy was constantly reflected between the grains and eventually consumed, resulting in the observed opacity.

1. Introduction

Optically transparent RE^{3+}-doped nanocrystal materials have attracted considerable attention for use in numerous photonic applications, such as optical fibres, solid lasers, three-dimensional displays and so on [1–6]. RE^{3+}-doped oxide glass ceramics possess excellent chemical and mechanical stability, but exhibit a high phonon energy which contributes to their poor optical performance. Fluoride glass ceramics can be doped with rare-earth ions and offer excellent transparency, rare earth ion solubility, and low phonon energy; however, such ceramics show a characteristic susceptible to corrosion and poor stability, which consequently have a negative influence on optical applications [7–9]. Some new transparent oxyfluoride glass ceramics, such as CaF$_2$, BaF$_2$, NaYF$_4$, LaF$_3$, etc., in which RE^{3+} are incorporated and dispersed within the glass matrix, offer an economical alternative with substantial performance improvement. This is because they commonly possess the optical advantages of pure fluoride glasses doped with rare earth irons, moreover, they have the thermal and mechanical advantages of oxide glasses [10,11].

Transparent glass ceramic preparation technology is based on controlling the heat treatment, namely, nucleation and crystallization of the base glasses, through which the nanocrystalline phase with a size of 5–100 nm is formed and embedded within the glass matrix. The CaF$_2$ crystal, an important small-size optical material, has a low melting point, and, meanwhile, acts as a nucleating agent, hence, the devitrification phenomenon occurs when the treatment temperature slightly exceeds the glass transition temperature. Subsequently, the crystals continues to increase in size until silicate crystalline phases of a large-size are generated [12,13]. Based on the Rayleigh scattering theory, for transparent photonic applications, the crystallite size must be much smaller than the wavelength of the incident light. In addition, the crystallites must be discretely distributed within the glass matrix to prevent light scattering [14–16]. Therefore, it is of interest and important to clarify the morphology and size of fluoride nanocrystals within the oxyfluoride crystallized glass, ensuring to obtain a transparent glass ceramic. There have been several reports on the non-isothermal crystallization of fluoride nanoparticles within transparent glass ceramics [17–21]. Rüssel [20,22] obtained CaF$_2$ nanocrystalline transparent glass ceramics with a crystal size of approximately 10 nm following heat-treatment between 520 °C and 560 °C. Similarly,

---

transparent products, embedded with BaF_2 nanocrystals with a crystal size of 6–15 nm, were also prepared via heat treatment performed between 500 °C and 600 °C. Both ceramics became opaque when the temperature was further increased. N. Hémono [17] also reported the development of transparent LaF_3-containing glass ceramics with a mean crystal size of 20 nm, which became opaque when the temperature was greater than 700 °C for 20 h. Based on the above reports, it can be determined that the spherical particles within these materials had an average size within the range of approximately tens of nanometres, which is far smaller than the wavelength of visible light. Hence, the conditions required for high transmittance are satisfied. However, there is no explanation for the change in the optical transmittance, such as from transparent to opaque, of these materials. Hence, in addition to the particle size factors, there are other factors that may affect the optical transmittance, which should be studied.

In the present work, the base glass, which contained CaF_2, was initially prepared following high temperature melting; the transparent glass ceramics were then produced via the crystallization of the base glass. The microstructure, transmittance, and mechanical properties of the obtained samples were analysed. The dependence of the mechanism associated with the optical transmittance of the material on the concentration of the precipitated CaF_2 nanocrystals was discussed in detail.

2. Experimental procedure

2.1. Synthesis of base glass

Based on previous studies [22,23], base glasses with a composition of $25CaF_2$-$40SiO_2$-$20Al_2O_3$-$7.5MgO$-$7.5CaO$ (mol%) were synthesized using a conventional melting-quenching method. Analytical grade MgO, Al_2O_3, SiO_2, CaF_2 and $CaCO_3$ were used as the raw materials. Typically, a sample batch, weighting 50 g, was thoroughly mixed and placed in a corundum crucible, and then melted at 1500 °C for 60 min in a high-temperature furnace for full melting. Subsequently, the melted solution was rapidly poured into a stainless steel mould, which had been previously preheated to 500 °C. This was then annealed at 500 °C for 180 min in a muffle furnace to release internal stress, and eventually cooled to room temperature, finally resulting in the preparation of a transparent and colourless base glass.

2.2. Preparation of transparent glass ceramic

The obtained base glasses were cut into pieces with dimensions of $20 \times 10 \times 1.5$ mm, and then subsequently subjected to a heat treatment process to prepare the transparent glass ceramics. The base glasses were each crystallized at temperatures of 630 °C, 670 °C, 700 °C, 730 °C, 740 °C, and 750 °C for a period of 1 h, 2 h, 3 h and 4 h. Eventually, the products were polished and prepared for subsequent characterization.

2.3. Characterization and measurement

The characteristic temperature of the base glass was determined by differential scanning calorimeter (DSC, STA409c, Germany). About 50 mg sample of the base glass powder was placed in a crucible and an empty crucible was used as a reference. The sample was then heated from room temperature to 1000 °C at a rate of 10 °C/min under an argon atmosphere.

The crystallization phases and particle sizes of all the synthesized samples were identified by the X-ray powder diffractometer (XRD, TTR3, Japan), using a Cu_α ($\lambda = 0.154$ nm) irradiation source operated at 30 kv, with a scan range of 10-90° and scan step of 0.02°/s.

A transmission electron microscope (TEM, JEM-2200FS, Japan), equipped with an energy dispersive X-ray spectroscopy system, and operated at an accelerating voltage of 200 kV, was used to assess the morphology and size of the CaF_2 nanoparticles within the crystallized ceramics.

To evaluate the molecular structure of the base glasses and heat-treated glass ceramics, Raman spectra measurements (Lab RAMHR Evolutio, France) were performed using the 532 nm line of a solid-state laser as the excitation source with the resolution of $0.65\ cm^{-1}$.

The light transmittance performance was investigated using an ultraviolet and visible spectrophotometer (TU-1901, China) over the range of 190 nm–900 nm, under a scanning speed of 240 nm/min. The light source is automatically converted pre-collimated deuterium lamp and iodine tungsten lamp.

With repared to the mechanical properties research, Vickers hardness (HV, 430SVD, USA) measurements were conducted under the load 1 N and holding time of 10 s. To determine the HV value, each sample was tested five times; the average value and standard deviation of the measurement were recorded.

3. Results and discussions

3.1. Characterization of the base glass

The base glass was prepared using a high-temperature melting, casting process, and a subsequent annealing process. To identify the phases and thermodynamic behaviour of the base glass, XRD and DSC experiments were performed, with the results shown in Fig. 1. It can be seen from the results that the as-obtained melted base glass is amorphous and visually colourless/transparent; moreover, as shown by the DSC results, the endothermic peaks representing the glass transition temperature, Tg (626.8 °C) and, melting temperature, Tm (972.1 °C), can be observed. An exothermic peak, representing the crystallization temperature, Tc (802.0 °C), can also be observed.

To obtain a transparent glass ceramic, it is necessary to hinder the generation of the main silicate phases, which easily results in glass devitrification, by controlling the heat treatment process. In addition, the nucleation temperature is typically 10 °C above the maximum glass transition temperature [20], so that the following heat treatment process was performed between 630 °C and 750 °C.

3.2. Characterization of the as-obtained transparent glass ceramics

Based on the above characterization of the base glass, the transparent glass ceramics were prepared using a heat treatment temperatures between 630 °C and 750 °C for periods of 1–4 h, with their characterization carried out as follows.

3.2.1. Phase analysis of the as-obtained transparent glass ceramics

The XRD patterns for the as-obtained glass ceramics are shown in
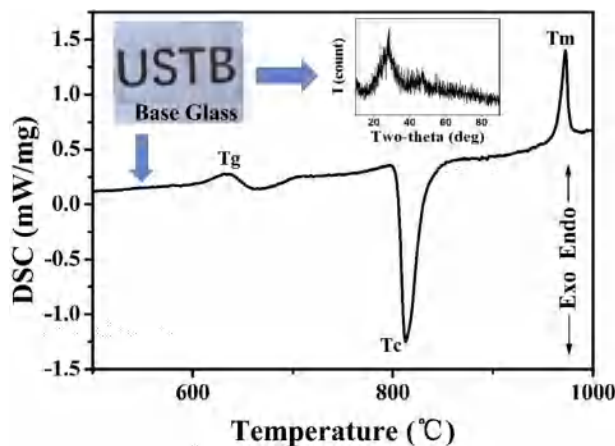
Fig. 1. The DSC curve obtained for the base glass sample with a heating rate 10 K/min under an argon atmosphere. The inset shows the amorphous X-ray pattern obtained for the base glass.
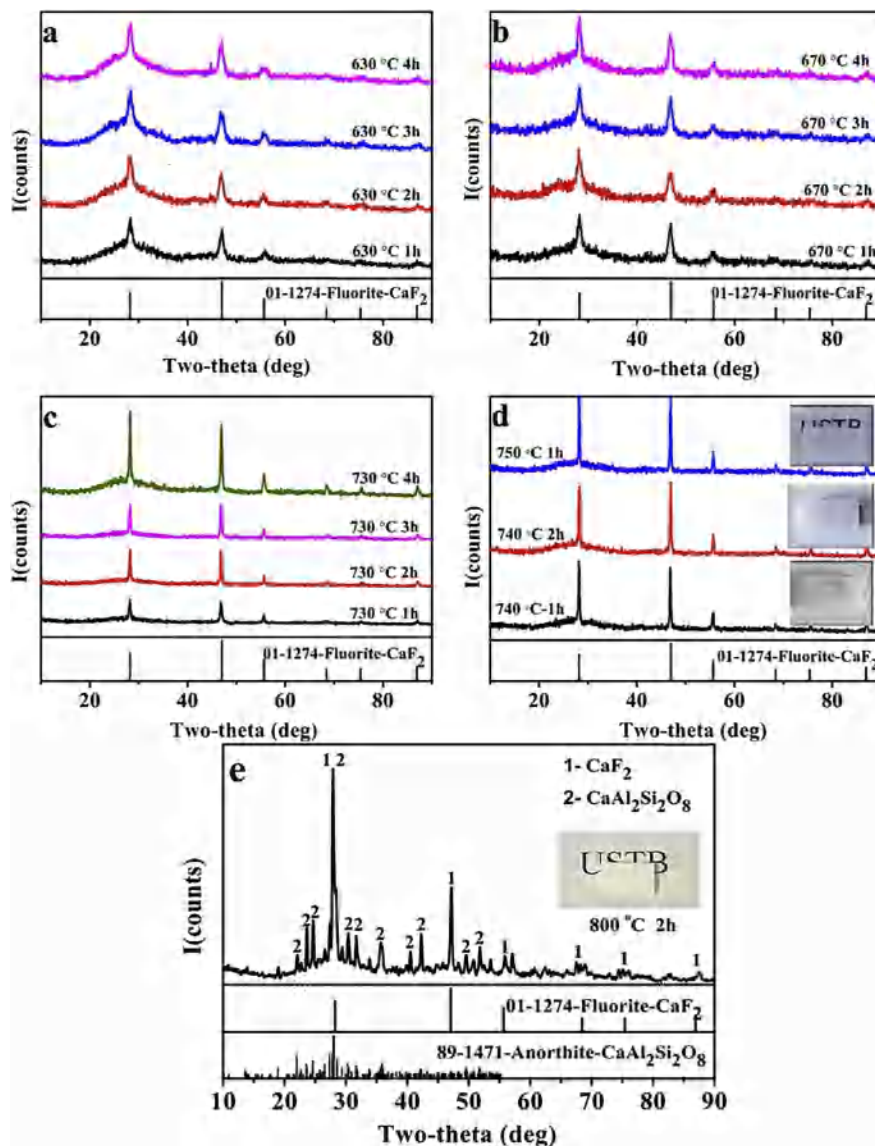
Fig. 2. XRD patterns of the crystallized samples that were annealed for 1–4 h under various heat treatment temperatures: (a) 630 °C, (b) 670 °C, (c) 730 °C, (d) 740 °C and 750 °C, (e) 800 °C.
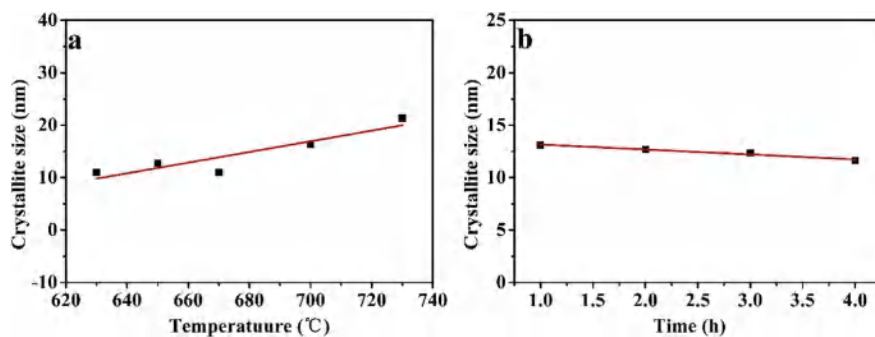
Fig. 3. Crystallite size of the formed CaF_2, as a function of (a) the heat treatment temperature the samples that was employed for 2 h, (b) the heat treatment period that was employed when the samples were treated at 670 °C.

Fig. 2. In the Fig. 2(a–d), following heat treatment, some distinct peaks, attributable to the crystalline phase of CaF_2 (JCPDF: 01-1274), can be observed at 28.217°, 47.045°, and 55.658°, respectively. As the heat treatment temperature increases from 630 °C to 750 °C under a consistent holding time, the crystalline peak strength becomes stronger and

sharper, indicating that the CaF_2 crystals also increases in size; however, almost all the crystal peaks are broadened, suggesting that the crystal size remains in a very small range. The variation tendency for prolonged heat treatment time of 1–4 h is relatively not obvious compared with that of the heat treatment temperature.

As shown in Fig. 2(e), when the as-obtained base glass is heat treated at 800 °C for 2 h, the glass ceramic become fully opaque. In addition to the diffraction peaks attributed to the generated CaF₂ crystals, some diffraction peaks attributed to the crystalline phase of CaAl₂Si₂O₈ (JCPDF: 89-1471) can be also observed. This phase is generated when the heat treatment temperature exceeds glass transition temperature (Tg) of 740 °C, through the thermodynamic behaviour of the base glass (Fig. 1), the CaAl₂Si₂O₈ crystals are formed in large quantities when the heat treatment temperature reaches the crystallization temperature (Tc).

Since the size of the generated CaF₂ nanocrystals varied with the heat treatment process, the XRD peak at approximately 47.045° was fitted using a Gauss curve, with the results presented in Fig. 3. The mean grain size of the crystalline CaF₂ phase was calculated using Scherrer's equation [24]:

$$d = \frac{G\lambda}{\beta \cos \theta} \tag{1}$$

where $G = 0.89$, d is the mean grain size, λ represents the wavelength of the X-ray radiation (Cu k_α = 0.154 nm), θ is the Bragg angle and β is the half width of the diffraction peak.

As shown in Fig. 3, the CaF₂ nanocrystal size lies in the range of 10–25 nm with heat treatment temperature increasing from 630 to 730 °C (Fig. 3(a)), however, it does not change significantly when the heat treatment period is further extended (Fig. 3(b)), which has been reported by other researchers [17,20]. It is clear that the nanocrystal size of the transparent glass ceramic is much smaller than the wavelength of visible light, and therefore, meets the requirements for Rayleigh scattering. However, when the transparent glass ceramic starts to become opaque when heat treated at 730 °C, the nanocrystal size of the material is still similar to those of the aforementioned transparent samples. This indicates that the nanocrystal size is not the only factor affecting the light transmittance.

According to previous reports [22], the concentration of generated CaF₂ nanocrystals increases as the heat treatment temperature is increased and period is extended, which may affect the light transmittance of transparent glass ceramics. To study the change rule for CaF₂ nanocrystal concentration, the area of the peak, which is proportional to the concentration of the formed crystalline CaF₂, at approximately 47.045° together with the FWHM are calculated [22] and the results are presented in Fig. 4. The larger the measured area is, the higher the concentration of CaF₂ nanocrystals generated. It can be seen that the concentration of the generated CaF₂ crystals proportionally increases with the heat treatment temperature (Fig. 4(a)) and period (Fig. 4(b)). This phenomenon is similar to those reported in previous studies, and may thus influence the light transmittance performance.

3.2.2. Micromorphology of the crystallized glass ceramics

The TEM micromorphology image of the obtained glass ceramic annealed at 670 °C for 2 h is presented in Fig. 5(a). The results show that there is a uniform and generous distribution of nanocrystals throughout the glass matrix. Regions A and B represent the nanocrystals and glass matrix, respectively. Fig. 5(b) reveals the crystal size distribution, which falls into a narrow range with an average grain size of 12 nm. There results correlate with the XRD results. The high resolution transmission electron microscope (HRTEM) image of a single grain was observed, as shown in the inset of Fig. 5(c), and used to calculate a d-spacing value of 0.269 nm, which could be attributed to the (220) plane of the CaF₂ crystals. To investigate the elemental distribution, the EDS spectra obtained for the CaF₂ crystals and glass matrix were studied, as shown in Fig. 5(c) and (d), respectively. It can be seen that the signal intensity for the F and Ca elements is stronger in the nanocrystals region and weaker in the glass matrix region.

3.2.3. Transmittance of the as-obtained transparent glass ceramics

Fig. 6 shows the transmittance curves obtained for the transparent glass ceramics prepared under various heat treatment conditions. When the heat treatment temperature is within the range of 630 °C–700 °C (Fig. 6(a–c)), the samples maintain excellent optical transparency, with the maximum transmittance remaining at approximately 85% in the visible light band, with almost all the light in the ultraviolet band absorbed. And the heat treatment period has little effect on the transmittance. When the heat treatment temperature is gradually increased to 730 °C, the samples start to become semi-transparent (Fig. 6(d)), with the transmittance in the visible light band showing a downward trend. When the heat treatment temperature is greater than 740 °C, the obtained samples become opaque and the transmittance is close to 0. In Fig. 3(e), it is comparatively obvious that the transmittance slightly decreases as the heat treatment temperature increases, especially when the glass ceramics initially become opaque.

Generally, in theory, with the increase of heat treatment time and temperature, the quantity of crystalline CaF₂ increases, which increases the light scattering and reduces the transmittance. However, as shown in Fig. 6(a–c), when the obtained glass-ceramics are transparent, the transmittance sometimes increases with heat treatment time, for example, the transmittance of the "700 °C, 3 h" sample is greater than that of the "700 °C, 1 h" sample. In addition to the experimental error factors (± 1.0%), the above phenomena may be due to the non-uniform crystallization, which results in variation of the transmittance.

3.2.4. Evaluation of mechanical properties

Fig. 7 shows the change in the microhardness value of the crystallized samples that were treated with temperature of 670 °C (dotted line) and heating period of 2 h (solid line), respectively. It can be seen that the average microhardness value of the crystallized glass is greater than that of the base glass, which also increases with increased heat treatment temperature and time. When the transparent glass ceramic was prepared at a temperature of 670 °C over a period of 4 h, the microhardness reached 761.62 ± 7.93 HV. This value is comparable to that of a spinel transparent glass ceramic based on the ZnO-Al₂O₃-SiO₂ system, which has a maximum microhardness value of 718 ± 4 HV [25]. Thus, the obtained transparent glass ceramics exhibit good
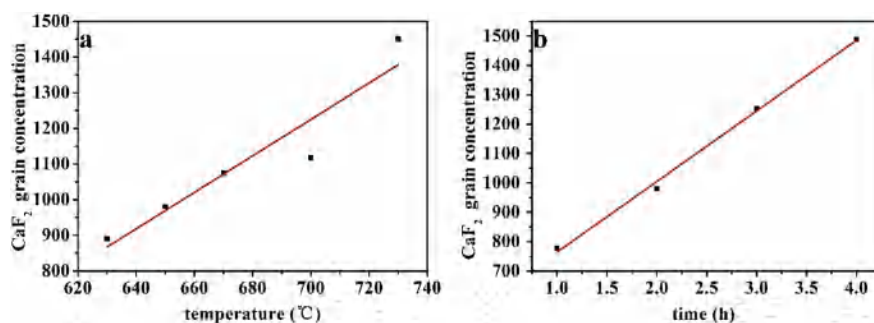
Fig. 4. CaF₂ grain concentration formed as a function of (a) the heat treatment temperature that was employed for 2 h, (b) the heat treatment period that was employed when the samples were treated at 670 °C.
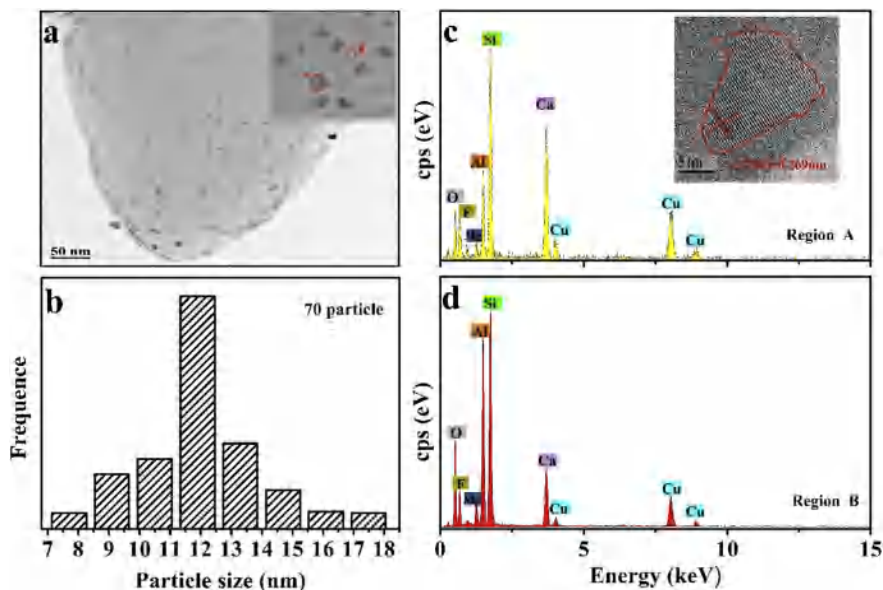
Fig. 5. (a) TEM micrograph of the obtained glass ceramic that was heat-treated at 670 °C for 2 h. (b) Crystal size distribution of the CaF_2 nanocrystals within the above glass ceramic. EDS spectra (c) obtained from an individual crystalline grain and (d) glass matrix shown in (a). The inset shown in (c) shows a high-resolution transmission electron microscope (HRTEM) image.
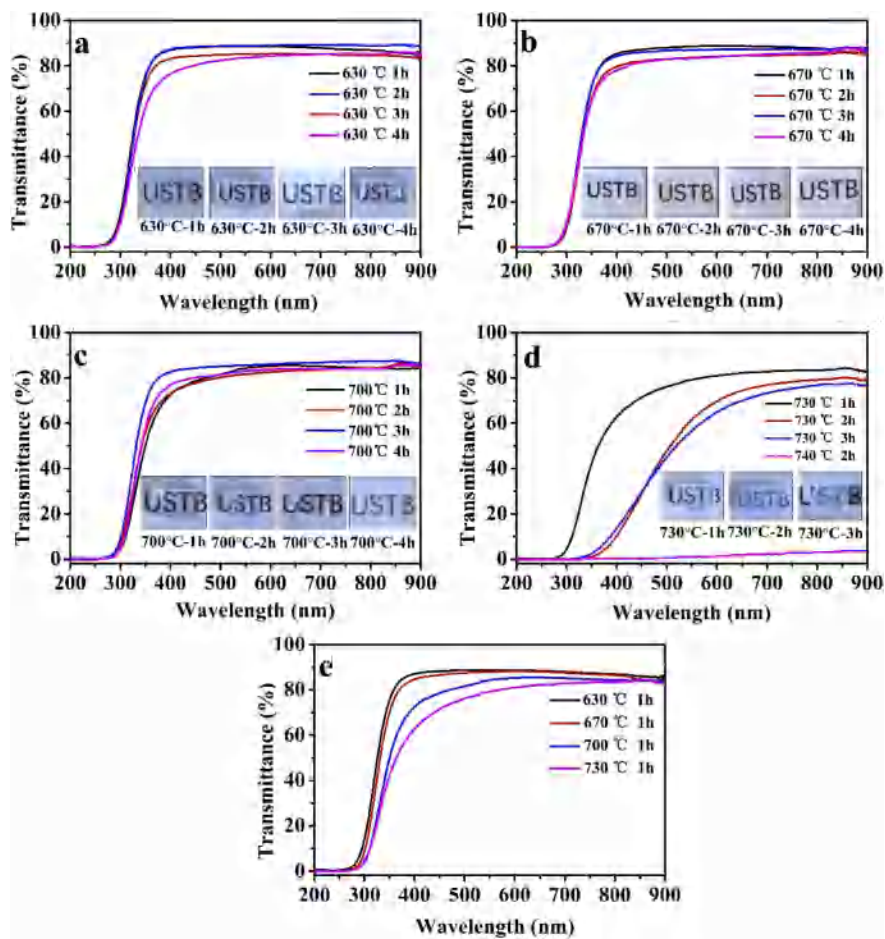
Fig. 6. Transmittance of the crystalized glass ceramic formed under various heat treatment conditions.

mechanical properties and can be applied in practical applications.

In summary, transparent CaF_2 nanocrystal glass ceramics were prepared under various heat treatment conditions using a conventional melting method. The preparation process is relatively simple and can be used for actual production. The transparent glass ceramics can remain transparent when heat-treated under temperatures between 630 °C and 700 °C for periods of 1–4 h, and gradually become opaque when the

temperature is increased above 730 °C for a period of 1 h. The precipitated CaF_2 nanocrystals are relatively uniformly distributed within the glass matrix. With increasing temperature and time, the CaF_2 grain concentration obviously increases; however, the grain size, which lies within the range of 10–25 nm, does not significantly change.
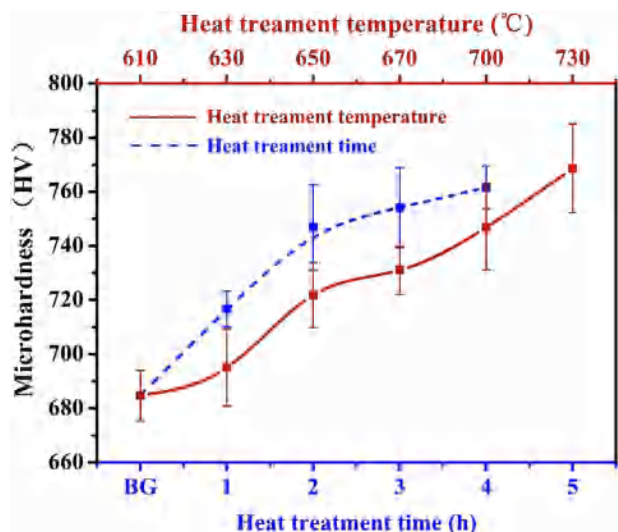
Fig. 7. The microhardness of the crystallized samples as a function of the heat treatment period employed at 670 °C (dotted line), and the heat treatment temperature used over a period of 2 h (solid line).

3.3. Mechanism associated with the light transmittance of the glass ceramics

In spite of the CaF_2 grain size being smaller than the wavelength of visible light, the obtained samples become opaque (Fig. 6(d)). Therefore, the grain size is no longer the only factor that has an influence on the transparency. It's important to consider the influence of the generated CaF_2 nanocrystal concentration on the light transmittance. This was fully studied through the analysis of the structure and morphology of the glass ceramics.

3.3.1. Molecular structure of the as-obtained glass ceramics

During the nucleation and crystallization process of CaF_2, the changes in the nanocrystals size and concentration are closely related to the molecular structure, which, hence, eventually affects the transmittance of the glass ceramics. To explore the effect of the grain concentration on the transmittance, Raman characterization was performed, with the results shown in Fig. 8. In Fig. 8(a), the band near 320 cm^{-1} is assigned to the vibration of the Ca-F bond [26,27], and its peak intensity increases with heat treatment temperature. Because the intensity of the Raman peak is connected to the content of the vibrational group, and the concentration of CaF_2 increases with heat treatment temperature, as calculated from the XRD results (Fig. 4), the vibration intensity of the glass ceramics increases with temperature, compared with the base glass without precipitated CaF_2 grains.

With the precipitation of the CaF_2 grains, the polymerization degree of the glass phase increases, along with the viscosity. These factors will influence the crystallization process, and, thus, lead to the concentration change of CaF_2 grains. Therefore, the molecular structure of the glass phase has been clarified in detail. Based on a previous Raman spectroscopy study of the structure of silicate and aluminosilicate glasses [28–32], the 400-600 cm^{-1} band is associated with flexural vibration owed to the bridging oxygen Si-O-Si. The band in the 800-1300 cm^{-1} region is thought to be due to the asymmetric vibration of the SiO_4 tetrahedron, where the specific peak wavenumber depends on the number of non-bridging oxygen (NBOs) and bridging oxygen (Q^i (si), i = 0,1,2,3) that constitute a tetrahedron. In particular, the band near 1050 cm^{-1} is attributed to the stretching vibration of a single NBOs Si-O in a tetrahedron (SiO_3O^-: Q^3), with the band near 960-980 cm^{-1} assigned to Si-O stretching with 2NBOs ($SiO_2O_2^{2-}$: Q^2). Similarly, the band near 900-930 cm^{-1} and 840-860 cm^{-1} represents the stretching vibration in silicate tetrahedral units with 3NBOs ($SiOO_3^{3-}$: Q^1) and 4NBOs (SiO_4^{4-}: Q^0), respectively. Gaussian functions were

applied to fit the Raman curves obtained for the samples, with the fitting results shown in Fig. 8(b)-(e). Subsequently, the mole fraction of the different structural units, i.e., Qi (Si), were calculated from the corresponding band area, with the change tendency for Qi (Si) shown in Fig. 8(f).

As shown in Fig. 8(f), with increasing heat treatment temperature, the mole fraction change trend for Q^2 does not obviously change. However, Q^3 increases, and, conversely, Q^1 decreases, with the change trend particularly evident when the transparent glass ceramics begin to become opaque when heat treated at 730 °C. The amount of bridging oxygen is the main factor affecting the integrity of the silicate structure in the glass ceramic: fewer bridge oxygens in the system correspond to a lower degree of structural integrity. For increasing heat treatment temperature from 630 to 730 °C, the CaF_2 nanocrystals are continuously precipitated from the glass matrix, meanwhile the content of $[SiO_4]$ and $[AlO_4]$ in the glass phase increases, leading to an increase in the number of bridge oxygens and complexity of the network structure. Therefore, the diffusion barrier becomes greater during the nucleation and subsequent crystal growth, which hinders further growth of the crystals [22]. When the heat treatment temperature reaches 730 °C, the mole fraction of Q^3 obviously increases, indicating that the viscosity of the glass phase increases significantly, with the concentration of the generated CaF_2 grains also increasing dramatically. This change trend may have affect the light scattering and eventually lead to the transparent glass ceramics becoming opaque.

Moreover, as shown in Fig. 7, the microhardness increases accordingly as the heat-treatment temperature increases and the treatment time is extended. The microhardness value of the glass ceramic is significantly related to its chemical bond strength and degree of structural integrity. The bridging oxygen bonds are stronger than the NBO bonds, besides, the hardness and strength of the material both increase as the network structure becomes more perfect [33,34]. Through structural analysis of as-obtained glass ceramics, as CaF_2 continues to form, the bridge oxygen bond and the degree of structural polymerization increases, which leads to an increase in microhardness. Therefore, this structural change eventually reflects the enhancement of the microhardness value of the glass ceramics with increasing heat treatment temperature and time.

3.3.2. Micromorphology of the transmittance glass ceramics

As discussed above, the CaF_2 nanocrystal concentration of the glass matrix will have a significant effect on the light scattering, and will result in varying transmittance values for the as-obtained glass ceramics. In this work, to better characterize the grains concentration, the concentration of CaF_2 nanocrystals is considered to be equivalent to the grain spacing between the neighbouring CaF_2 grains. The CaF_2 nanocrystals concentration decreases as the grain spacing increases. First, TEM measurements were performed on the obtained glass ceramics and the results are shown in Fig. 9. Subsequently, the centre of a single-crystal and its surrounding grains is determined, and then the grain spacing between two neighbouring crystals is measured as the distance from the surface of this single grain to that of the neighbouring grains.

The micrographs, shown in Fig. 9(a) ∼ (d), of the precipitated nanocrystals within the glass matrix that were annealed for 2 h at 630 °C, 670 °C, 700 °C, and 730 °C, respectively, were examined. The images portray monodisperse grains, which are uniformly embedded within the glass matrix. Moreover, it can be clearly observed that the crystal quantity increases as the heat treatment temperature increases.

The measured distance between grains was plotted in a histogram and shown in Fig. 9(e) ∼ (h), with the change in average grain spacing with heat treatment temperature also shown in Fig. 9(m). The results obviously show that the average grain spacing decreases with the improvement of heat treatment temperature. When the nucleation temperature increases from 630 °C to 700 °C, the average grain spacing reduces from 25.74 to 11.89 nm, with the glass ceramics obtained being transparent, indicating that the CaF_2 nanocrystal quantity in this range
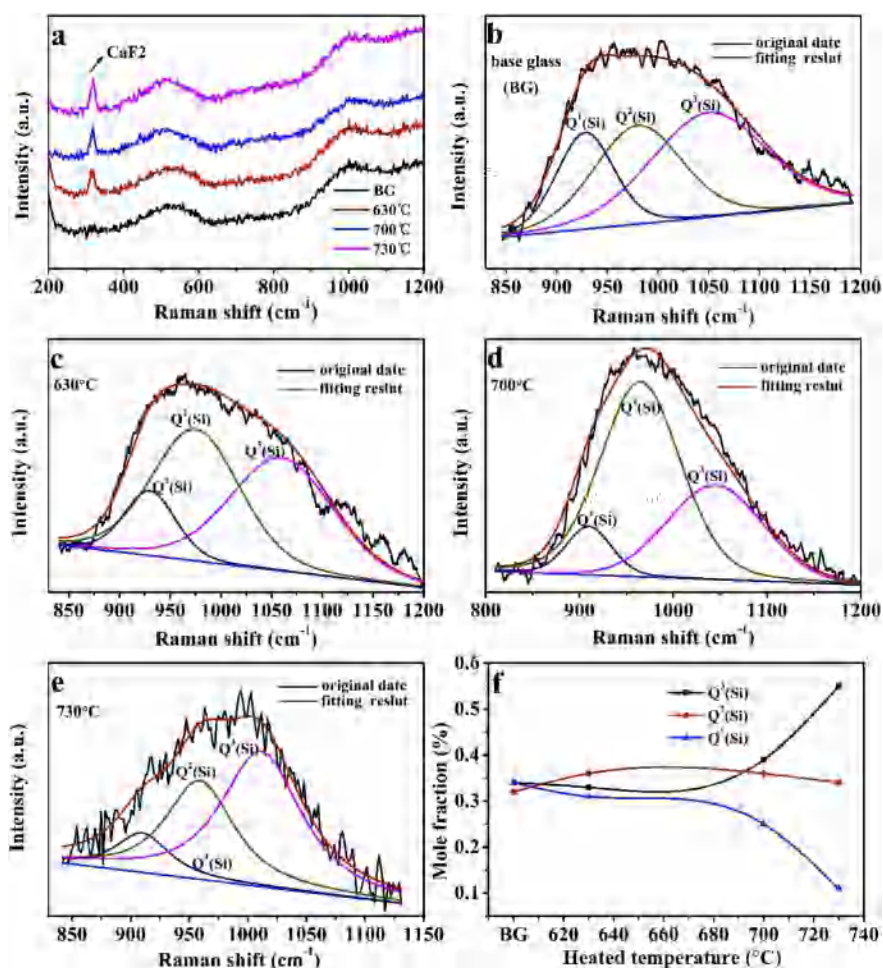
Fig. 8. Raman spectroscopy results obtained for the non-annealed sampled and the samples that were annealed at various temperature for 2 h. (a) General Raman spectra of the samples. (b) ~ (e) The unfolding result of Raman peak of samples at 0 °C, 630 °C, 700 °C, 730 °C respectively. (f) The mole fraction of Q^i (i = 1.2.3) as a function of the heat treatment temperature.

has little effect on light scattering, with most of the incident light passing through the glass ceramic. When the glass ceramics are in a semi-transparent state, heat-treated at 730 °C, the mean grain spacing decreases to approximately 5.64 nm, indicating that part of the light energy is consumed through mutual refraction between the nanocrystals, with only part of the incident light passing through the glass ceramics. When the temperature increases to 740 °C, the glass ceramics begin to become opaque, with the corresponding micrograph shown in Fig. 9(k). In this case, the precipitated CaF_2 nanocrystals embedded in the glass matrix are distributed close to each other, with the average grain spacing obviously much less than 5 nm. Consequently, the energy of all the incident light will be gradually consumes in the mutual refraction between the internal grains, resulting in light being unable to penetrate the samples [35,36]. Based on the above analysis, it is obvious that the mean grain spacing of the CaF_2 nanocrystals has a major effect on the light transmittance of the transparent glass ceramics.

Generally, in this work, CaF_2 transparent glass ceramics were prepared using a conventional melting process with a heat treatment temperature between 630 °C and 730 °C. In the case of the as-obtained transparent glass ceramics, the grain size should be much smaller than the wavelength of visible light; in addition, the mean grain spacing can also influence the light transmittance. The size of the precipitated CaF_2 nanocrystals should within the range of 10–25 nm, and the mean grain spacing should be greater than 5.64 nm.

4. Conclusions

In this study, a transparent glass ceramic based on CaF_2 nanocrystals was controllably synthesized via a melting process and subsequent heat treatment. By analysing of structures and morphologies of the samples, the mechanism associated with the transition of the glass ceramic from a transparent to an opaque state was further clarified. In general, transparent CaF_2 glass ceramics can be prepared when heat treated between 630 °C and 730 °C. These materials have a CaF_2 grain size of 10–25 nm and an average grain spacing greater than 5.64 nm. With regard to the wavelength region of visible light, the transmittance of the transparent glass ceramics exceeds 80%. When the temperature exceeds 730 °C, the transparent glass ceramics start to become opaque, with the average grain spacing decreasing to less than 5 nm. The Raman results show that the polymerization degree of the glass ceramics increases with the heat treatment temperature, especially when the temperature reaches 730 °C. The significant increase in the degree of polymerization indicates that there is an increase in the viscosity of the glass phase and a significant increase in the concentration of the formed CaF_2 nanocrystals. This has a greater impact on the light scattering, and thus affects the transmittance of the transparent glass ceramics. In general, the nanocrystal size and mean grain spacing are two factors that affect the transmittance of the transparent glass ceramics.
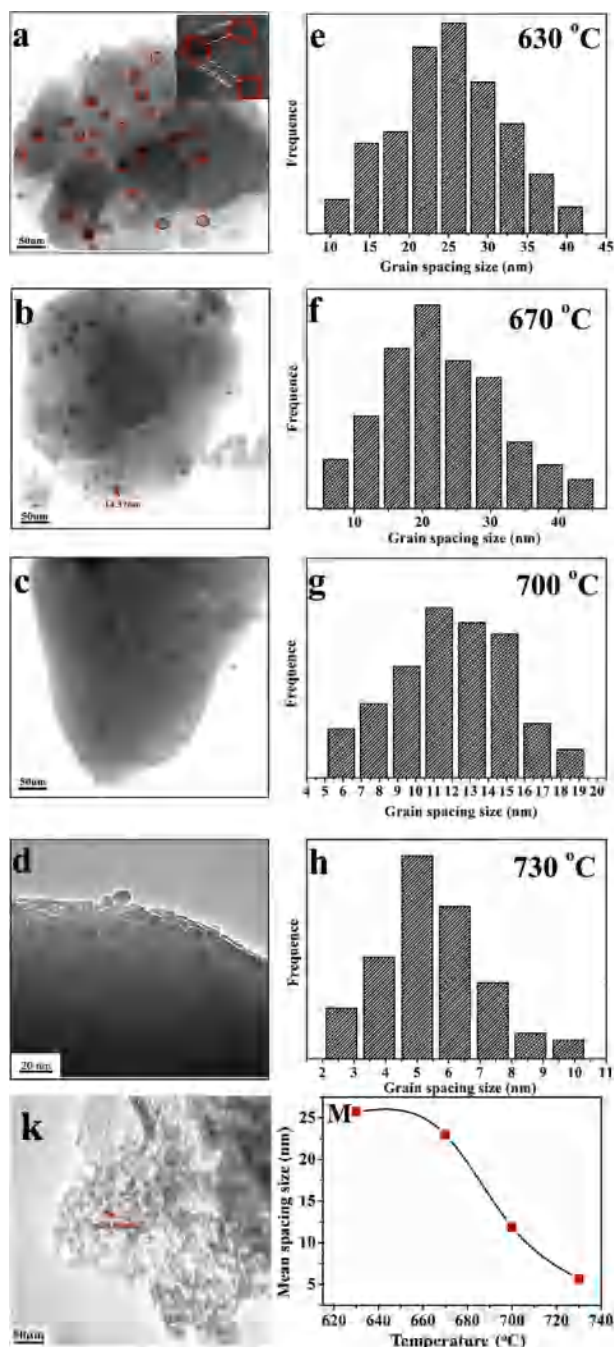
Fig. 9. TEM micrographs of the precipitated nanocrystals of the glass ceramics that were heated for 2 h at (a) 630 °C, (b) 670 °C, (c) 700 °C, (d) 730 °C, (k) 750 °C. (e)–(h) Columnar distribution map of the adjacent grain spacing measurements corresponding with (a) to (d). (m) Average spacing as a function of the heat treatment temperature.

References

[1] E. Downing, L. Hesselink, et al., A three-color, solid-state, three-dimensional display, Science 273 (1996) 1185–1189.

[2] G. Yi, H. Lu, S. Zhao, et al., Synthesis characterization, and biological application of size-Controlled nanocrystalline NaYF4:Yb, Er infrared-to-visible up-conversion phosphors, Nano Lett. 4 (2004) 2191–2196.

[3] F. Weng, D. Chen, et al., Energy transfer and up-conversion luminescence in Er/Yb co-doped transparent glass ceramic containing YF nano-crystals, Ceram. Int. 35 (2009) 2619–2623.

[4] D. Chen, Y. Chen, Transparent Ce^{3+}: $Y_3Al_5O_{12}$ glass ceramic for organic-resin-free white-light-emitting diodes, Ceram. Int. 40 (2014) 15325–15329.

[5] Y. Gao, Y. Hu, D. Zhou, et al., Effect of crystalline fraction on upconversion luminescence in Er^{3+}/Yb^{3+} Co-doped $NaYF_4$ oxyfluoride glass-ceramics, J. Eur. Ceram. Soc. 37 (2017) 763–770.

[6] X. Liu, J. Zhou, S. Zhou, et al., Transparent glass-ceramics functionalized by dispersed crystals, Prog. Mater. Sci. 97 (2018) 38–96.

[7] L. Xiao, W. Wang, H. Gao, et al., Synthesis and optical properties of Bi^{3+}/Yb^{3+} co-doped transparent oxyfluoride glass–ceramics, Ceram. Int. 41 (2015) 10137–10141.

[8] B. Derkowska-Zielinska, L.W. Yu, et al., Optical characterisation of Er^{3+}-doped oxyfluoride glasses and nano-glass-ceramics, Mater. Lett. 136 (2014) 233–236.

[9] A.J. Stevenson, H. Serier-Brault, et al., Fluoride materials for optical applications: single crystals, ceramics, glasses, and glass-ceramics, J. Fluorine Chem. 132 (2011) 1165–1173.

[10] Y. Jiang, J. Fan, et al., Structure and optical properties of transparent Er^{3+}-doped CaF_2-silica glass ceramic prepared by controllable sol-gel method, Ceram. Int. 42 (2016) 9571–9576.

[11] A.D. Pablosmartín, A. Durán, et al., Nanocrystallisation in oxyfluoride systems: mechanisms of crystallisation and photonic properties, Int. Mater. Rev. 57 (2012) 165–186.

[12] G. Aldica, M. Secu, Investigations of the non-isothermal crystallization of CaF_2, nanoparticles in Sm-doped oxy-fluoride glasses, J. Non-Cryst. Solids 356 (2010) 1631–1636.

[13] K. Shinozaki, T. Honma, et al., Morphology of CaF_2 nanocrystals and elastic properties in transparent oxyfluoride crystallized glasses, Opt. Mater. 33 (2011) 1350–1356.

[14] P.P. Fedorov, A.A. Luginina, et al., Transparent oxyfluoride glass ceramics, J. Fluorine Chem. 172 (2015) 22–50.

[15] S. Hendy, Light scattering in transparent glass ceramics, Appl. Phys. Lett. 81 (2002) 1171–1173.

[16] T. Berthier, V.M. Fokin, E.D. Zanotto, New large grain, highly crystalline, transparent glass-ceramics, J. Non-Cryst. Solids 354 (2008) 1721–1730.

[17] N. Hémono, G. Pierre, F. Muñoz, et al., Processing of transparent glass-ceramics by nanocrystallisation of LaF_3, J. Eur. Ceram. Soc. 29 (2009) 2915–2920.

[18] J. Cai, X. Wei, F. Hu, et al., Up-conversion luminescence and optical thermometry properties of transparent glass ceramics containing CaF_2:Yb^{3+}/Er^{3+} nanocrystals, Ceram. Int. 42 (2016) 13990–13995.

[19] J. Fan, S. Chen, X. Yuan, et al., Recrystallization of Er^{3+}: CaF_2 in transparent fluorophosphate glass-ceramics with the Co-firing method, J. Am. Ceram. Soc. 99 (2016) 2971–2976.

[20] C. Bocker, C. Rüssel, Self-organized nano-crystallisation of BaF_2 from NaO/KO/ BaF/AlO/SiO glasses, J. Eur. Ceram. Soc. 29 (2009) 1221–1225.

[21] F. Muñoz, A.D. Pablos-Martín, N. Hémono, et al., NMR investigation of the crystallization mechanism of LaF_3 and $NaLaF_4$ phases in aluminosilicate glasses, J. Non-Cryst. Solids 357 (2011) 1463–1468.

[22] C. Rüssel, Nanocrystallization of CaF_2 from Na_2O/K_2O/CaO/CaF_2/Al_2O_3/SiO_2 glasses, Chem. Mater. 17 (2005) 5843–5847.

[23] C. Bocker, S. Bhattacharyya, et al., Size distribution of BaF_2 nanocrystallites in transparent glass ceramics, Acta Mater. 57 (2009) 5956–5963.

[24] Y. Gao, Y. Hu, et al., Effect of Li^+ ions on the enhancement upconversion and Stokes emission of $NaYF_4$: Tb, Yb co-doped in glass-ceramics, J. Alloy. Comp. 667 (2016) 297–301.

[25] A.J. Stryjak, P.W. Mcmillan, Microstructure and properties of transparent glass-ceramics, J. Mater. Sci. 13 (1978) 1275–1281.

[26] M. Grimsditch, M. Cardona, et al., Resonance in the Raman scattering of CaF_2, SrF_2, BaF_2 and diamond, J. Raman Spectrosc. 10 (1981) 77–81.

[27] R. Srivastava, L.L. Chase, et al., Raman frequencies of fluorite crystals ☆, Phys. Lett. 36 (1971) 333–334.

[28] S. Agathopoulos, D.U. Tulyaganov, et al., Structural analysis and devitrification of glasses based on the CaO–MgO–SiO_2 system with B_2O_3, Na_2O, CaF_2, and P_2O_5 additives, J. Non-Cryst. Solids 352 (2006) 322–328.

[29] Bjørn O. Mysen, David Virgo, Interaction between fluorine and silica in quenched melts on the joins SiO_2-AlF_3 and SiO_2-NaF determined by Raman spectroscopy, Phys. Chem. Miner. 12 (1985) 77–85.

[30] T. Furukawa, K.E. Fox, W.B. White, Raman spectroscopic investigation of the structure of silicate glasses. III. Raman intensities and structural units in sodium silicate glasses, J. Chem. Phys. 75 (1981) 3226–3237.

[31] B.O. Mysen, L.W. Finger, D. Virgo, et al., Curve-fitting of Raman spectra of silicate glasses, Am. Mineral. 67 (1982) 686–695.

[32] P. Colomban, H.D. Schreiber, Raman signature modification induced by copper nanoparticles in silicate glass, J. Raman Spectrosc. 36 (2010) 884–890.

[33] G. Bartenev, The structure and strength of glass fibers, J. Non-Cryst. Solids 1 (1968) 69–90.

[34] G. Kaur, O.P. Pandey, K. Singh, Effect of modifiers field strength on optical, structural and mechanical properties of lanthanum borosilicate glasses, J. Non-Cryst. Solids 358 (2012) 2589–2596.

[35] S. Hendy, Light scattering in transparent glass ceramics, Appl. Phys. Lett. 81 (2002) 1171–1173.

[36] B. Xia, X. He, D. Sun, et al., The electrically controlled light scattering performances of PLZT transparent ceramics, Ceram. Int. 41 (2015) S246–S249.